Int. J. Appl. Math. Comput. Sci., 2025, Vol. 35, No. 3, 455–466
DOI: 10.61822/amcs-2025-0032

CONSTRUCTION AND DEFORMATION OF CURVES AND SURFACES BASED ON α–SH BASIS FUNCTIONS WITH SHAPE PARAMETERS

KEWEI ZHANG [a], HAN WANG [a,*]

[a]School of Computer Science and Technology
Shandong Technology and Business University
No. 191, Binhai Middle Road, Laishan District, Yantai, Shandong, 264003, China
e-mail: 2022410070@sdtbu.edu.cn,wanghan19881214@126.com

Curve and surface modeling techniques have long been essential in computer graphics research. However, many existing methods for curve and surface fitting, as well as deformation, have limitations, such as challenges in representing certain special curve forms and a lack of control over the deformation process. Therefore, there is a need for a method that accurately represents specific curves and surfaces while allowing for a more intuitive and straightforward deformation implementation. To address this, the paper proposes a new method for constructing curves and surfaces and for their deformation. First, a shape-controlled basis function, termed the α-sh basis function, is defined in the basis vector space $\{1, t, t^2, \ldots, t^{n-2}, \sinh t, \cosh t\}$. Next, the favorable properties of the α-sh basis function are analyzed and proven, demonstrating its feasibility for curve and surface fitting. Using this basis function, α-sh Bézier curves and $\alpha\beta$-sh Bézier surfaces are defined, and their properties are thoroughly analyzed and proven. Finally, by adjusting the shape control parameters, the deformation of curves and surfaces can be achieved. The proposed method also enables the representation of special curves, such as circles, and allows for their deformation. The paper concludes with examples of curves and surfaces, visualizations of their deformation effects, and potential applications in practical industrial design.

Keywords: hyperbolic sine function, curve and surface construction, shape parameter, deformation technique.

1. Introduction

Curves and surfaces are fundamental elements in computer-aided design (Kennard and Stone, 1969; Ross and Rodriguez, 1963; Narayan *et al*., 2008) and geometric modeling (Mortenson, 1997; Farin *et al*., 1987). The study of curves and surfaces involves expressing complex shapes, making it a crucial area within computer graphics. Bézier curves and surfaces are commonly used construction methods in this field (Marschner and Shirley, 2018; 2009; Foley *et al.*, 1994; Kotan *et al.*, 2021). These methods are easy to understand and implement, and they exhibit desirable smoothness properties. However, once the control points and Bernstein basis functions of traditional Bézier curves and surfaces are defined, their shapes become fixed. This characteristic leads to a high degree of rigidity, so adjusting the position of a single control point can result in substantial changes to the overall shape, thereby limiting shape manipulation capabilities. Additionally, in industrial design, scenarios often arise involving circles, spheres, and other geometric forms, where traditional Bézier curves and surfaces are inadequate.

To achieve surface deformation, Barr (1984) proposed an innovative approach for both global and local deformation of 3D objects, effectively handling conventional deformations such as twisting, stretching, and compression. However, it has limitations in performing arbitrary rotations. In 1986, Sederberg and Parry (1986) introduced Free-Form Deformation (FFD), a technique that embeds a 3D geometric model into a spatial grid and deforms the model by altering the shape of the grid. This method has been widely applied and extended in various fields, including computer graphics, CAD, animation, simulation, and medical image processing. Hsu *et al*. (1992) proposed a method that allows users to directly manipulate points to deform a surface, eliminating the need for a detailed understanding of the surface construction. This approach simplifies the

*Corresponding author

deformation process. Building upon FFD, Bechmann *et al*. (1997) introduced additional control points, enabling users to more precisely control the deformation area, facilitating the creation of more complex shapes. However, these techniques face challenges in terms of spatial and temporal complexity, which has led to the development of more direct methods for curve and surface deformation.

In recent years, an increasing number of scholars have incorporated shape parameters into the construction of basis functions for curve and surface deformation. Qin *et al*. (2013) introduced a novel polynomial basis function with $n-1$ local shape control parameters, enabling the construction of Bézier curves with n local shape control parameters. They analyzed the properties of these basis functions, discussed various curve design applications, and demonstrated the impact of control parameters on curve shapes. Said Mad Zain *et al*. (2021) proposed a generalized fractional-order Bézier curve with shape and fractional parameters, exploring the influence of these parameters on curve shape and continuity in piecewise curves. Wen-tao and Guo-zhao (2005) designed an expandable λ-Bézier surface using a set of control planes with λ-Bézier basis functions, which incorporate shape parameters. Ameer *et al*. (2022) proposed a new formula for designing curves and surfaces, extending the application of Bézier curves and surfaces. By adjusting these parameters, the surface shape can be modified, and they discussed the properties and potential applications of the surface.

The methods mentioned above all use Bernstein basis functions to construct curves, but they still have limitations in representing certain special curves. To address these limitations, research on alternative basis functions has emerged. Shen and Wang (2015) introduced a Bézier curve based on trigonometric functions, demonstrating the construction of special curves using C-Bézier bases. Yang and Zeng (2009) and Maqsood *et al*. (2020) added two shape control parameters to these trigonometric Bézier bases, analyzing the continuity and geometric properties of the curves, and discussing the design and application of various curves and surfaces.

The methods described above exhibit favorable properties in curve construction and deformation; however, they also have certain limitations, such as difficulties in representing special curves and achieving simplicity and controllability in the deformation process. Additionally, some of these construction methods are restricted to low-dimensional curve construction and have not been extended to surface construction.

This paper proposes a new basis function for constructing curves and surfaces, derived through integration to create a function space based on hyperbolic sine functions, which incorporates shape parameters. This new basis function construction method outperforms traditional polynomial basis functions in constructing special curves and surfaces. It not only enables the construction of special curves, such as circles, but also allows for shape control of curves and surfaces through shape parameters. The deformation process becomes more intuitive as it does not require changing the control points. In Section 2, we present the construction of the basis function with shape control parameters, analyze its properties, and prove its feasibility in geometric shape generation. In Sections 3 and 4, we use this basis function to fit curves and surfaces, analyze the properties of the constructed curves and surfaces, and provide simple examples to illustrate the impact of shape control parameters on the deformation of curves and surfaces. In Section 5, we demonstrate the practicality of surface deformation in real-world applications.

2. Construction and properties of α-sh basis functions

The core of curve and surface design lies in the construction of basis functions. Below, the construction of the α-sh basis function is presented, and its properties are analyzed.

2.1. Basis function α-sh. To achieve more direct and flexible curve deformation, the vector space spanned by $\{1, t, t^2, \ldots, t^{n-2}, \sinh t, \cosh t\}$ is extended with shape control parameter α, allowing for precise control over the deformation of the curve.

Definition 1. The n-th order α-sh basis function is denoted as $b_{i,n}(t)$, where $i = 0, 1, \ldots, n$. When $n = 1$, two initial basis functions are obtained:

$$\begin{aligned} b_{_{0,1}}(t) &= \frac{\sinh \alpha(1-t)}{\sinh \alpha}, \\ b_{_{1,1}}(t) &= \frac{\sinh \alpha t}{\sinh \alpha}, \end{aligned} \tag{1}$$

where $\alpha \in (0, +\infty), t \in [0, \alpha]$.
For $n > 1$, the basis function $\{b_{0,n}, b_{1,n}, \ldots, b_{n,n}\}$ is recursively defined in the vector space $\{1, t, t^2, \ldots, t^{n-2}, \sinh t, \cosh t\}$ as follows:

$$\begin{aligned} b_{0,n} &= 1 - \int_0^t \delta_{0,n-1} b_{0,n-1}(s)\,\mathrm{d}s, \\ b_{i,n} &= \int_0^t (\delta_{i-1,n-1} b_{i-1,n-1}(s) \\ &\quad -\delta_{i,n-1} b_{i,n-1}(s))\,\mathrm{d}s, \\ b_{n,n} &= \int_0^t \delta_{n-1,n-1} b_{n-1,n-1}(s)\,\mathrm{d}s, \end{aligned} \tag{2}$$

where

$$\delta_{i,n} = \frac{1}{\int_0^\alpha b_{i,n}(t)\mathrm{d}t}, \quad 0 < i < n.$$

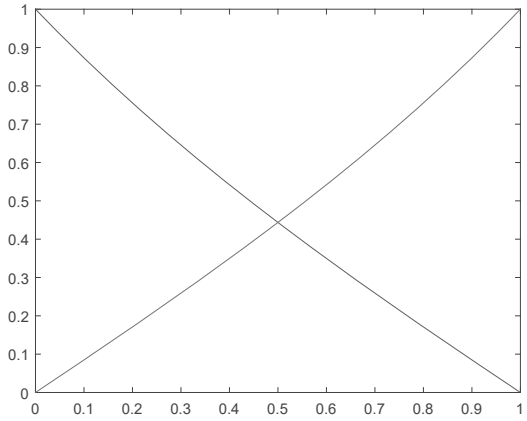

Fig. 1. Basis functions of 2nd-order for $\alpha = 1$.

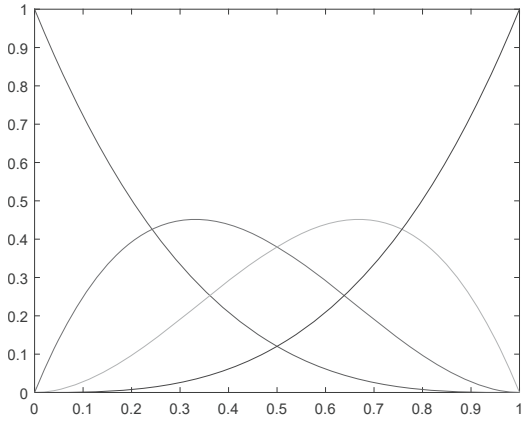

Fig. 2. Basis functions of 4th-order for $\alpha = 1$.

We obtain the definition of the α-sh basis functions, where α is referred to as the shape parameter.

Using the basis function expressions, we obtain the graphs of the basis functions when the parameter $\alpha = 1$. Below are two examples.

Example 1. The graphs of 2nd-order basis functions: formula with the basis functions 3 are presented in Fig. 1.

$$\begin{cases} b_{01} = \frac{\sinh(1-t)}{\sinh 1}, \\ b_{11} = \frac{\sinh t}{\sinh 1}, \end{cases} \qquad t \in [0,1]. \tag{3}$$

♦

Example 2. Figure 2 presents the graphs of the 4th-order basis functions. ♦

From Figs. 1 and 2, we can preliminarily observe some excellent properties of the α-sh basis functions. The graphs are all positioned in the positive direction of the y-axis, ensuring the non-negativity of the basis functions. The graphs are very smooth, with no discontinuities, guaranteeing the accuracy of curve and surface construction. The boundary values are either 0 or 1, determining the weight of the boundary points, which is important for boundary control. In the following, we will analyze and prove more of these properties.

2.2. Properties of the α-sh basis function. In the following, we provide a detailed analysis and prove the good properties of the α-sh basis function.

Property 1. (*Normalization*) The sum of the values of all α-sh basis functions is always 1 over the interval $[0, \alpha]$, i.e.,

$$\sum_{i=1}^{n} b_{i,n}(t) = 1, \quad t \in [0,\alpha], \quad \alpha \in (0,+\infty). \tag{4}$$

Proof. The 2nd-order basis function can only construct simple line segments, so we will consider higher-order cases. When $n >1$, we have

$$\begin{aligned} \sum_{i=1}^{n} b_{i,n}(t) &= b_{0,n}(t) + b_{1,n}(t) + \ldots \\ &\quad + b_{n-1,n}(t) + b_{n,n}(t) \\ &= \left(1 - \int_0^t \delta_{0,n-1} b_{0,n-1}(s)\,\mathrm{d}s\right) \\ &\quad + \Big(\int_0^t \big(\delta_{0,n-1} b_{0,n-1}(s) \\ &\quad - \delta_{1,n-1} b_{1,n-1}(s)\big)\,\mathrm{d}s\Big) \\ &\quad + \ldots \\ &\quad + \left(\int_0^t \delta_{n-2,n-1} b_{n-2,n-1}(s)\,\mathrm{d}s\right) \\ &\quad - \left(\int_0^t \delta_{n-1,n-1} b_{n-1,n-1}(s)\,\mathrm{d}s\right) \\ &\quad + \left(\int_0^t \delta_{n-1,n-1} b_{n-1,n-1}(s)\,\mathrm{d}s\right) \\ &= 1. \end{aligned} \tag{5}$$

■

Property 2. (*Endpoint characteristics*) Only the first and last α-sh basis functions take the value of 1 at their respective endpoints, while the other basis functions take the value of 0 at these endpoints. When $t = 0$, $b_{0,n}(0) = 1, \quad b_{i,n}(0) = 0 \quad \text{for} \quad i > 0$. When $t = 1$, $b_{n,n}(1) = 1$, $b_{i,n}(1) = 0 \quad \text{for} \quad i < n$.

Proof. From the definition of the basis functions, it is clear that this property holds when $n = 1$. When $n > 1$,

Substituting into Definition 1 and simplifying, we obtain

$$\begin{aligned}
b_{0,n}(0) &= 1 - \int_0^0 \delta_{0,n-1} b_{0,n-1}(s)\,\mathrm{d}s = 1,\\
b_{n,n}(\alpha) &= \int_0^\alpha \delta_{n-1,n-1} b_{n-1,n-1}(s)\,\mathrm{d}s\\
&= \delta_{n-1,n-1}\int_0^\alpha b_{n-1,n-1}(s)\,\mathrm{d}s\\
&= \delta_{n-1,n-1}\cdot\frac{1}{\delta_{n-1,n-1}} = 1,\\
b_{i,n}(0) &= \int_0^0 \delta_{i-1,n-1} b_{i-1,n-1}(s)\\
&\quad - \delta_{i,n-1} b_{i,n-1}(s)\,\mathrm{d}s = 0,\\
b_{i,n}(\alpha) &= \int_0^\alpha \delta_{i-1,n-1} b_{i-1,n-1}(s)\\
&\quad - \delta_{i,n-1} b_{i,n-1}(s)\,\mathrm{d}s\\
&= \delta_{i-1,n-1}\cdot\frac{1}{\delta_{i-1,n-1}}\\
&\quad - \delta_{i,n-1}\cdot\frac{1}{\delta_{i,n-1}} = 0.
\end{aligned} \tag{6}$$

■

Property 3. (*Linear independence*) A set of basis functions $\{b_1(t), b_2(t), \ldots, b_n(t)\}$ is linearly independent on the interval $[0, \alpha]$ if and only if the following condition holds:

$$c_1 b_1(t) + c_2 b_2(t) + \cdots + c_n b_n(t) = 0 \quad \text{for all } t \in [0,\alpha], \tag{7}$$

where the only solution is $c_1 = c_2 = \cdots = c_n = 0$, then the set of basis functions is linearly independent.

Proof. Assume that there exists a non-trivial solution to the equation $\sum_{i=0}^{n} a_i b_{i,n}(t) = 0$. That is the functions $b_{i,n}(t)$ are linearly dependent. Let $t = 0$. From the endpoint characteristics of the basis functions, it follows that $a_0 = 0$. Next, differentiating both sides of the equation $\sum_{i=0}^{n} a_i b_{i,n}(t) = 0$ i times with respect to t, we can successively conclude, using the endpoint properties of the basis functions, that $a_i = 0$ for all i. This leads to a contradiction of the assumption that there is a non-trivial solution; therefore, the functions $b_{i,n}(t)$ are linearly independent. ■

Property 4. (*Positivity*) The basis functions $\{b_1(t), b_2(t), \ldots, b_n(t)\}$ satisfy the positivity property if

$$b_i(t) \geq 0, \quad \forall t \in [0,\alpha], \quad \text{for all } i = 1, 2, \ldots, n.$$

Proof. Assume that $b_{i,n}(t)$ has $n+1$ zeros. By Rolle's Theorem, $b_{i,n}(t)$ must be n-times differentiable, which would contradict the linear independence of the basis functions. Therefore, $b_{i,n}(t)$ can have at most n zeros. Combining this with Property 3, we can conclude that $b_{i,n}(t)>0$ for all relevant t. ■

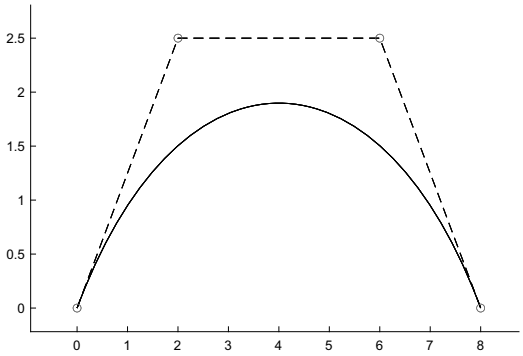

Fig. 3. Bézier α-sh curve (solid line) and its control polygon (dashed line) when $\alpha = 1$.

3. Bézier α-sh curve

Once the n-th order α-sh basis functions are determined, a curve segment can be obtained by linearly combining the basis functions with $n+1$ control points.

3.1. Construction curve. In the following, we present the construction of the α-sh Bézier curve and provide a simple example to illustrate the curve.

Definition 2. Assume that $P_i \in \mathbb{R}^d$ $(d = 2, 3)$ for $i = 0, 1, \ldots, n$, is a set of control points. Let the n-th order basis functions be denoted by $b_{i,n}(t)$, where $i = 0, 1, \ldots, n$. The curve $C(t)$ can then be expressed using these basis functions, as follows:

$$C(t) = \sum_{i=0}^{n} b_{i,n}(t) P_i, \quad t \in [0,\alpha], \quad \alpha \in (0, +\infty). \tag{8}$$

Example 3. (*Continuation of Example 2*) Given a set of control points in two-dimensional space

$$P_0(0,0), P_1(2,2.5), P_2(6,2.5), P_3(8,0).$$

The basis functions obtained in Example 2, when the control points are substituted into Eqn. 8, yield the curve $C_1(t)$. Specifically, $C_1(t) = P_0 b_{03}(t) + P_1 b_{13}(t) + P_2 b_{23}(t) + P_3 b_{33}(t)$. As shown in Fig. 3, the solid curve represents $C_1(t)$, the circles indicate control points, and the dashed line represents the control polygon. Figure 2 shows the basis functions corresponding to the curve.

♦

It is evident from Fig. 3 that the curve has desirable properties, including endpoint characteristics, the convex hull property, and convexity preservation. The following sections provide an analysis and proof of these properties.

3.2. Properties of the curve. In the following, we provide a detailed analysis and prove the good properties of the α-sh Bézier curve.

Property 5. (*Endpoint characteristics*)

$$C(0) = \sum_{i=0}^{n} b_{i,n}(0)P_i, C(\alpha) = \sum_{i=0}^{n} b_{i,n}(\alpha)P_i.$$

Proof. From the endpoint characteristics of the α-sh basis functions, it can be concluded that $C(0) = P_0, C(\alpha) = P_n$.

■

Property 6. (*Differentiation properties*) Differentiating the n-th order α-sh Bézier curve, we obtain

$$C^{'}(t) = \sum_{i=0}^{n-1} b_{i,n-1}(t)Q_i, \quad t \in [0, \alpha], \quad \alpha \in (0, +\infty), \tag{9}$$

where $Q_i = \delta_{i,n-1}(P_{i+1} - P_i)$.

Proof. Assume that the curve $C(t)$ is an $(n+1)$-th order curve:

$$C'(t) = P_0(b_{0,n}(t))' + P_1(b_{1,n}(t))' + \ldots + P_i(b_{i,n}(t))' + \ldots + P_n(b_{n,n}(t)') \tag{10}$$

By substituting Eqn. (2) into Eqn. (10), we obtain

$$\begin{aligned} C'(t) = {} & P_0\left(-\delta_{0,n-1}b_{0,n-1}(t)\right) \\ & + P_1\left(\delta_{0,n-1}b_{0,n-1}(t) - \delta_{1,n-1}b_{1,n-1}(t)\right) \\ & + \ldots + P_i\left(\delta_{i-1,n-1}b_{i-1,n-1}(t)\right. \\ & \left.-\delta_{i,n-1}b_{i,n-1}(t)\right) \\ & + \ldots + P_n\left(\delta_{n-1,n-1}b_{n-1,n-1}(t)\right). \end{aligned}$$

It can be simplified to

$$\begin{aligned} C^{'}(t) = {} & \delta_{0,n-1}(P_1 - P_0)b_{0,n-1}(t) \\ & + \cdots + \delta_{i,n-1}(P_{i+1} - P_i)b_{i,n-1}(t) \\ & + \cdots \delta_{n-1,n-1}(P_n - P_{n-1})b_{n-1,n-1}(t) \\ = {} & \sum_{i=0}^{n-1} \delta_{i,n-1}b_{i,n-1}(t)Q_i, \end{aligned}$$

where $Q_i = P_{i+1} - P_i$. ■

Property 7. (*Convex hull property*) It follows from the normalization and non-negativity of the α-sh basis functions that the α-sh Bézier curve always lies within the control polygon formed by the control points.

Property 8. (*Variation diminishing property*) The number of intersections between any plane and the α-sh Bézier curve is at most equal to the number of intersections between the plane and the associated control polygon.

Proof. Assume that a line L intersects both the curve $C(t)$ and the control polygon of the curve, with m intersection points between L and $C(t)$. These m points divide the segments of the control polygon into several parts. By geometric properties, L will intersect each segment of the control polygon at most once. Since the curve is contained within the convex hull of the control polygon, L is guaranteed to intersect $C(t)$ at least once on each segment of the control polygon. Thus, the number of intersections between L and the curve $C(t)$ cannot exceed the number of intersections between L and the control polygon.

■

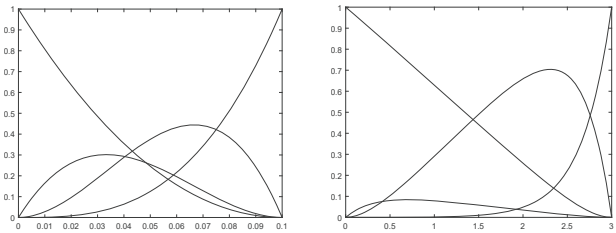

(a) (b)

Fig. 4. Comparison of α-sh basis functions with changing parameters: α-sh basis function when $\alpha = 0.1$ (a), α-sh basis function when $\alpha = 3$ (b).

Property 9. (*Convex preservation of the curve*) Due to the variation-reduction property of α-sh Bézier curves, it can be concluded that if the control polygon is convex, the corresponding curve will also be convex.

3.3. Deformation control of α-sh Bézier curves by parameters. After defining the α-sh Bézier curve, this section presents a simple example to demonstrate how the shape control parameter affects the curve. The parameter α influences the values of the basis functions across their domain as its magnitude changes. As the magnitude of α changes, the weight associated with the corresponding control point P_i also changes, resulting in a variation in the curve's shape.

Example 4. (*Continuation of Example 2*) The effect of changes in the shape parameter on the basis function is shown in Fig. 4.

Comparing the basis function shown in Fig. 2, Fig. 4(a) illustrates that as the shape parameter decreases, the weights of the first and second control points among the four control points decrease, causing the curve to move away from the control edge P_0P_1. Figure 4(b) shows that as the shape parameter increases, the weights of the first and third control points increase, while the weights of the second and fourth control points decrease, pulling the curve closer to P_2. The specific influence of the shape parameter on the curve shape is shown in Fig. 5.

♦

After analyzing the properties and deformation control of the α-sh Bézier curve, it is demonstrated that the curve has a simple construction, predictable shape,

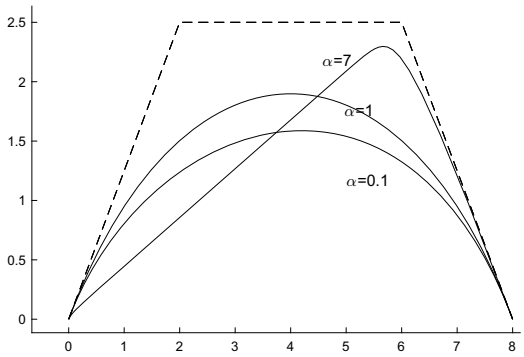

Fig. 5. Bézier α-sh curve (solid line) corresponding to different values of the α parameter.

smoothness, and strong continuity. Furthermore, by introducing a shape control parameter, the curve's shape can be adjusted without altering the positions of the control points, providing enhanced controllability.

4. Bézier $\alpha\beta$-sh surface

After obtaining the α-sh Bézier curve, the $\alpha\beta$-sh Bézier surface can be considered as the product of two α-sh Bézier curves.

4.1. Definition of the surface. Next, we present the construction of the $\alpha\beta$-sh Bézier surface and provide a simple example to illustrate the surface.

Definition 3. Given a set of $(m+1)\times(n+1)$ spatial control points P_{ij}, the surface is defined as a linear combination of these control points, weighted by the α-sh basis functions through the tensor product, and is expressed as

$$S(u,v;\alpha,\beta)=\sum_{i=0}^{m}\sum_{j=0}^{n}b_{i,m}(u)b_{j,n}(v)P_{ij},\quad u\in[0,\alpha],\ v\in[0,\beta],\ \alpha,\beta\in(0,+\infty). \tag{11}$$

The surface is denoted as $S(u,v)$, where P_{ij} are the control points, and $b_{i,m}(u)$ and $b_{j,n}(v)$ are the α-sh basis functions in the u and v directions, respectively. Once the surface is constructed, the parameters α and β can be adjusted in both directions to achieve surface deformation.

Example 5. Assuming the surface S_1 is fitted from 16 points, the basis functions are consistent with Example 2, and the surface is represented as

$$S_1(u,v)=\sum_{i=0}^{3}\sum_{j=0}^{3}b_{i,3}(u)b_{j,3}(v)P_{ij},$$

$$S_1(u,v)=\sum_{i=0}^{3}\sum_{j=0}^{3}b_{i,3}(u)b_{j,3}(v)P_{ij}=UPV,$$

where

$$U=(b_{0,3}(u),b_{1,3}(u),b_{2,3}(u),b_{3,3}(u)),$$
$$V=(b_{0,3}(v),b_{1,3}(v),b_{2,3}(v),b_{3,3}(v))^{\mathsf{T}}.$$

The control point matrix P is

$$\begin{pmatrix}(0,0,0)&(1,0,1)&(2,0,1)&(3,0,0)\\(0,1,1)&(1,1,2)&(2,1,2)&(3,1,1)\\(0,2,1)&(1,2,2)&(2,2,2)&(3,2,1)\\(0,3,0)&(1,3,1)&(2,3,1)&(3,3,0)\end{pmatrix}.$$

The surface $S_1(t)$ and its control mesh are shown in Fig. 6(a), while Fig. 6(b) displays the basis functions in both directions for the surface. As shown in Fig 6(a), the $\alpha\beta$-sh Bézier surface possesses boundary properties, corner point properties, and convex hull properties. The following sections will analyze and prove these properties. ♦

4.2. Properties of the surface. In the following, we provide a detailed analysis and prove the good properties of the $\alpha\beta$-sh Bézier surface.

Property 10. (*Boundary properties*) The boundary curves of the surface can be defined as

$S(0,v)$ is the α-sh Bézier curve defined by the points $P_{0,j}$,
$S(\alpha,v)$ is the α-sh Bézier curve defined by the points $P_{m,j}$,
$S(u,0)$ is the α-sh Bézier curve defined by the points $P_{i,0}$,
$S(u,\beta)$ is the α-sh Bézier curve defined by the points $P_{i,n}$.

Property 11. (*Corner property*) When u and v take the values 0 and α (for u) and 0 and β (for v), the $\alpha\beta$-sh Bézier surface produces the corner points of the surface, as follows:

$$S(0,0)=P_{0,0},S(0,\beta)=P_{0,n},$$
$$S(\alpha,0)=P_{m,0},S(\alpha,\beta)=P_{m,n}.$$

Property 12. (*Convex hull property*) The $\alpha\beta$-sh Bézier surface is a convex combination of control points and always lies within the convex hull formed by these control points.

Property 13. (*Separability*) The $\alpha\beta$-sh Bézier surface can be expressed as the outer product of two α-sh Bézier curves:

$$S(u,v)=C_u(t)\times C_v(t),$$

allowing for independent manipulation along the u and v components.

Property 14. (*Variation diminishing*) In an $\alpha\beta$-sh Bézier surface, the number of intersection points between any plane and the surface does not exceed the number of intersection points with its control mesh. This property ensures that the surface can effectively control deformation during shape changes while maintaining smoothness and continuity.

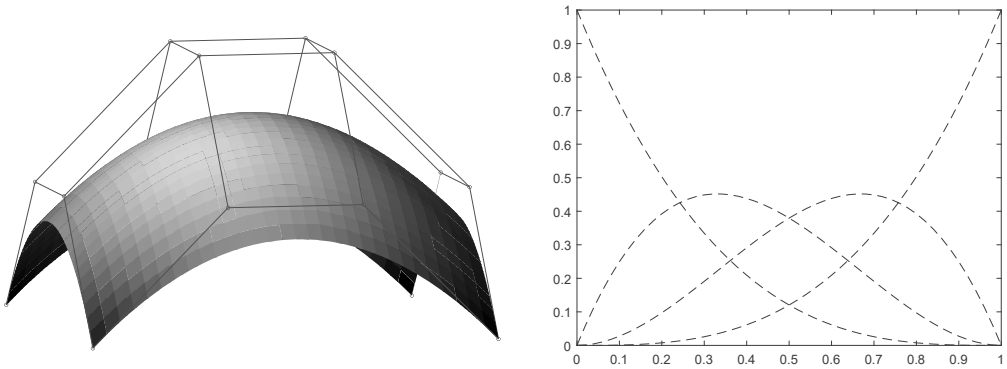

(a) (b)

Fig. 6. Bézier $\alpha\beta$-sh surface when $\alpha = 1$: $\alpha\beta$-sh Bézier surface and control mesh (a), α-sh basis function (b).

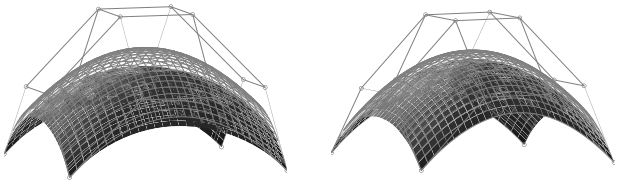

(a) (b)

Fig. 7. Surface with decreased shape parameters on different components: $\alpha, \beta = 0.1$ (a), $\alpha = 1, \beta = 0.1$ (b).

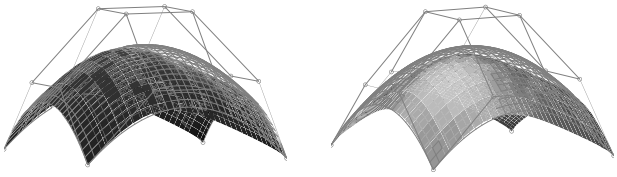

(a) (b)

Fig. 8. Surface with increased shape parameters on different components: $\alpha = 1$, $\beta = 3$ (a), $\alpha = 3$, $\beta = 3$ (b).

4.3. Parameter control for $\alpha\beta$-sh Bézier surfaces deformation. After defining the $\alpha\beta$-sh Bézier surface, its construction involves two parameters, α and β, which correspond to the two directions introduced by the increase in dimensions. Similar to the shape control principle for curves, α and β serve as shape control parameters. When their values change, the values of the basis functions within their respective domains also change. As the magnitudes of $b_{i,m}(t)$ and $b_{j,n}(t)$ vary, the weights at the control points P_{ij} are modified, leading to the desired shape transformation. This section illustrates the impact of these shape parameters on the surface through an example.

Example 6. According to the separability property of the surface, the shape parameters in the u and v directions can be adjusted independently, altering the weights of the control points along each direction. The effects of changing the shape parameters on the basis functions are illustrated in Figs. 4(a) and 4(b).

In Figs. 7 and 8, the mesh represents the surface's position when both α and β are equal to 1. In Fig. 7(a), when both α and β are simultaneously reduced, the entire surface, except for the corner points, moves away from the control mesh. In Fig. 7(b), when only β is changed, the boundary curves corresponding to α on the surface remain unchanged, while the surface moves away from the control mesh in the β direction. In Fig. 8(a), when only β increases, the surface moves closer to the previous endpoint in the β direction, while the boundary curves corresponding to α remain unchanged. In Fig. 8(b), when the parameters in both directions are increased, the surface moves towards the previous endpoint in both dimensions, pulling it toward one corner. ♦

From the analysis of the surface properties and the shape control demonstrated in Example 3, it is evident that the $\alpha\beta$-sh Bézier surface is simply constructed and exhibits good stability. By introducing control parameters, both the overall contour and the local shape of the surface can be adjusted with greater precision. The positions of the start and end points, together with the shape control parameters, enable fine-tuning of the surface. This flexibility allows for various shape deformations by increasing or decreasing the shape control parameters, thereby improving design efficiency.

5. Application

Based on the principles of curve and surface construction and deformation, this section presents several application examples.

When connecting multiple curves, certain conditions must be satisfied to ensure better continuity. Suppose there is a curve C_1, constructed with three control points

P_0, P_1, and P_2, and another curve C_2, constructed with three control points P_3, P_4, and P_5. When point P_2 coincides with point P_3, the curves C_1 and C_2 are G^0-continuous at the point of coincidence. The two curves are abbreviated as $C_1 = P_0 b_{0,2} + P_1 b_{1,2} + P_2 b_{2,2}$, $C_2 = P_3 b_{0,2} + P_4 b_{1,2} + P_5 b_{2,2}$. To ensure that the two curves are G^1-continuous, their tangent directions at the point of coincidence must be the same and proportional. It satisfies the following formula:

$$\frac{\mathrm{d}\mathbf{t}}{\mathrm{d}C_1} = c \cdot \frac{\mathrm{d}\mathbf{t}}{vC_2}.$$

.

By Property 6, we obtain

$$C_1' = \delta_{0,1}(b_{0,1})(P_1 - P_0) + \delta_{1,1}(b_{1,1})(P_2 - P_1),$$

$$C_2' = \delta_{0,1}(b_{0,1})(P_4 - P_3) + \delta_{1,1}(b_{1,1})(P_5 - P_4).$$

By solving the above three equations simultaneously, we obtain

$$P_1 - P_0 = \zeta(P_4 - P_3),$$

$$P_2 - P_1 = \zeta(P_5 - P_4),$$

where ζ is an arbitrary constant.

5.1. Deformation of α-sh Bézier curves.

Example 7. Constructing a circle. A single Bézier curve cannot precisely define a closed shape, such as a circle. To address this, four control points are used to fit a quarter-circle arc. These four arc segments are then joined together to form a complete circle. Finally, a shape control parameter is applied to deform the circle.

Based on the definition of the α-sh Bézier curve and the tangent directions at the start and end points of the arc, we begin by assuming the positions of the control points as follows:

$$P_0\,(r,0)\,, P_1\,(r,d)\,, P_2\,(d,r)\,, P_3\,(0,r)\,.$$

To refine these positions, we represent the arc as a standard Bézier curve:

$$C(t) = P_0(1-t)^3 + P_1 \cdot 3(1-t)^2 t + P_2 \cdot 3(1-t)t^2 + P_3 \cdot t^3.$$

When $t = 0.5$, the corresponding point on the arc is $\left(\frac{\sqrt{2}}{2}, \frac{\sqrt{2}}{2}\right)$. This gives the equation

$$\left(\frac{\sqrt{2}}{2}, \frac{\sqrt{2}}{2}\right) = \frac{1}{8}(r,0) + \frac{3}{8}(r,d) + \frac{3}{8}(d,r) + \frac{1}{8}(0,r).$$

Solving this, we get

$$d = r \cdot \frac{4}{3}\tan\left(\frac{\pi}{8}\right).$$

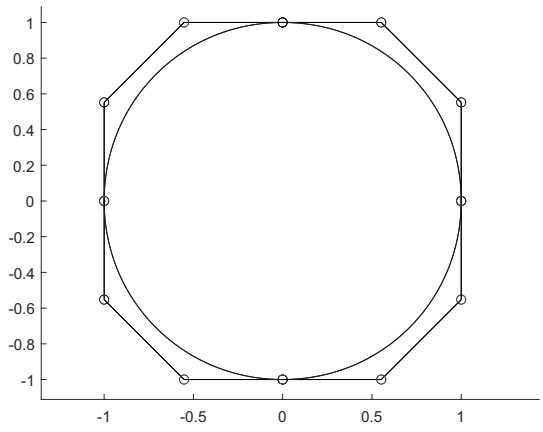

(a)

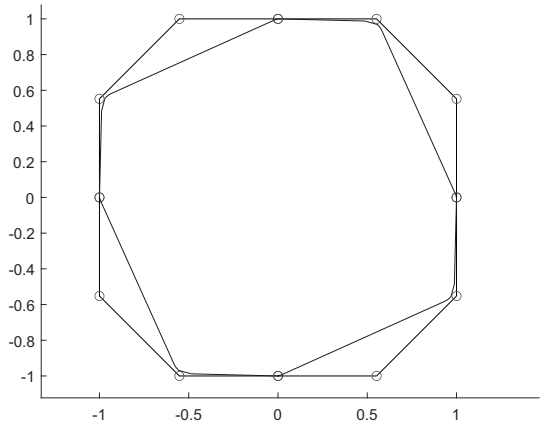

(b)

Fig. 9. Changes in the circle when the shape parameter increases: $\alpha = 0.975$ (a), $\alpha = 10$ (b).

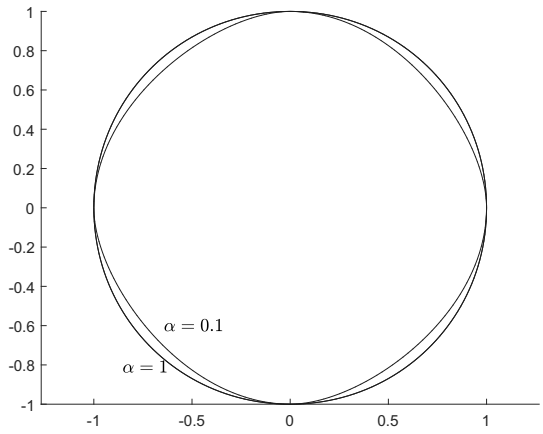

Fig. 10. Changes in the curve when the shape parameter α decreases.

Let $k = \frac{4}{3}\tan\left(\frac{\pi}{8}\right)$ (in the following text, k will denote this value). Then, four sets of control points are used to construct the circle. The coordinates of the control points are as follows (where r is the radius of the circle):

$$\{(r,0),(r,r\cdot k),(r\cdot k,r),(0,r)\},$$

$$\{(0,r),(-r\cdot k,r),(-r,r\cdot k),(-r,0)\},$$

$$\{(-r,0),(-r,-r\cdot k),(-r\cdot k,-r),(0,-r)\},$$

$$\{(0,-r),(r\cdot k,-r),(r,-r\cdot k),(r,0)\}.$$

By adjusting the parameters simultaneously, a circle (Fig. 9(a)) can be obtained when the parameter $\alpha = 0.975$.

As the parameter increases, the curve is pulled toward the control point immediately before the endpoint.

As the parameter decreases, it can be observed from Fig. 10 that the fitted curve, except at the endpoints, moves away from the control polygon. ♦

Example 8. A three-dimensional spiral curve is fitted in three-dimensional space based on a two-dimensional circle, using four sets of control points. Figure 11 illustrates how the spiral curve changes as the parameters vary. The control points are as follows:

$$\{(6,0,0),(6,6\cdot k,1),(6\cdot k,6,2),(0,6,3)\},$$

$$\{(0,6,3),(-6\cdot k,6,4),(-6,6\cdot k,5),(-6,0,6)\},$$

$$\{(-6,0,6),(-6,-6\cdot k,7),(-6\cdot k,-6,8),(0,-6,9)\},$$

$$\{(0,-6,9),(6\cdot k,-6,10),(6,-6\cdot k,11),(6,0,12)\}.$$

♦

5.2. Deformation of the $\alpha\beta$-sh Bézier surface. After applying the curve, we extend the dimensions to apply the circle to a surface.

Example 9. Building on the 3D spiral curve, we extend it into a 3D spiral surface by connecting four adjacent surface segments. Each segment is defined by a set of control points in three-dimensional space, as shown below:

$$\begin{pmatrix} (6,0,0) & (3,0,0) & (0,0,0) \\ (6,6\cdot k,1) & (3,3\cdot k,1) & (0,0,1) \\ (6\cdot k,6,2) & (3\cdot k,3,2) & (0,0,2) \\ (0,6,3) & (0,3,3) & (0,0,3) \end{pmatrix},$$

$$\begin{pmatrix} (0,6,3) & (0,3,3) & (0,0,3) \\ (-6\cdot k,6,4) & (-3\cdot k,3,4) & (0,0,4) \\ (-6,6\cdot k,5) & (-3,3\cdot k,5) & (0,0,5) \\ (-6,0,6) & (-3,0,6) & (0,0,6) \end{pmatrix},$$

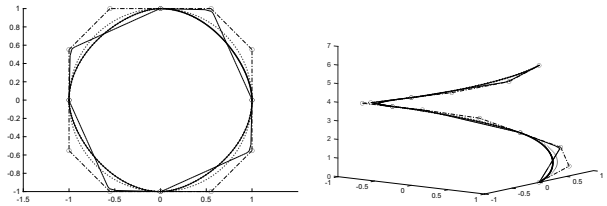

(a) (b)

Fig. 11. Spirals with the dotted line for $\alpha = 0.975$, dash-dotted line for $\alpha = 0.1$, solid line for $\alpha = 10$. Top view of the spiral (a), 3D view of the spiral (b).

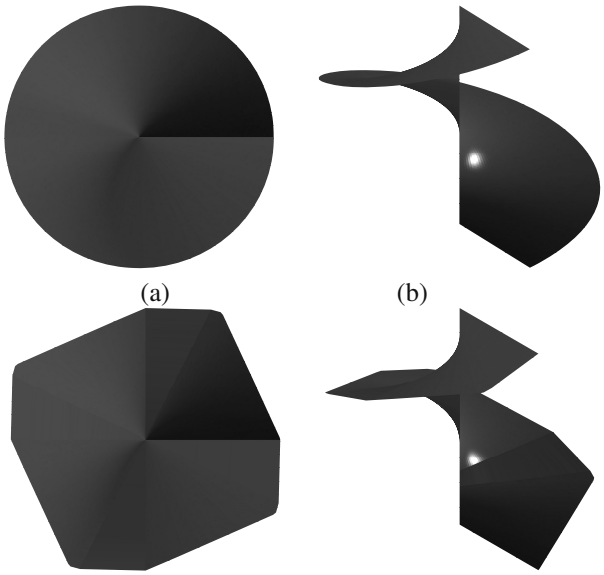

(a) (b) (c) (d)

Fig. 12. Spiral surfaces with different parameters: top view of the spiral surface when $\alpha = 0.975$ (a), spiral surface when $\alpha = 0.975$ (b), top view of the spiral surface when $\alpha = 10$ (c), spiral surface when $\alpha = 10$ (d).

$$\begin{pmatrix} (-6,0,6) & (-3,0,6) & (0,0,6) \\ (-6,-6\cdot k,7) & (-3,-3\cdot k,7) & (0,0,7) \\ (-6\cdot k,-6,8) & (-3\cdot k,-3,8) & (0,0,8) \\ (0,-6,9) & (0,-3,9) & (0,0,9) \end{pmatrix},$$

$$\begin{pmatrix} (0,-6,9) & (0,-3,9) & (0,0,9) \\ (6\cdot k,-6,10) & (3\cdot k,-3,10) & (0,0,10) \\ (6,-6\cdot k,11) & (3,-3\cdot k,11) & (0,0,11) \\ (6,0,12) & (3,0,12) & (0,0,12) \end{pmatrix}.$$

Here, we use four control points. Along the direction of the control points aligned with the parameter β, all control points lie on a straight line, meaning that variations in β do not affect the surface shape. Only the parameter α influences the surface geometry. Figure 12 shows the surface shapes for different values of α, with Fig. 12(c)

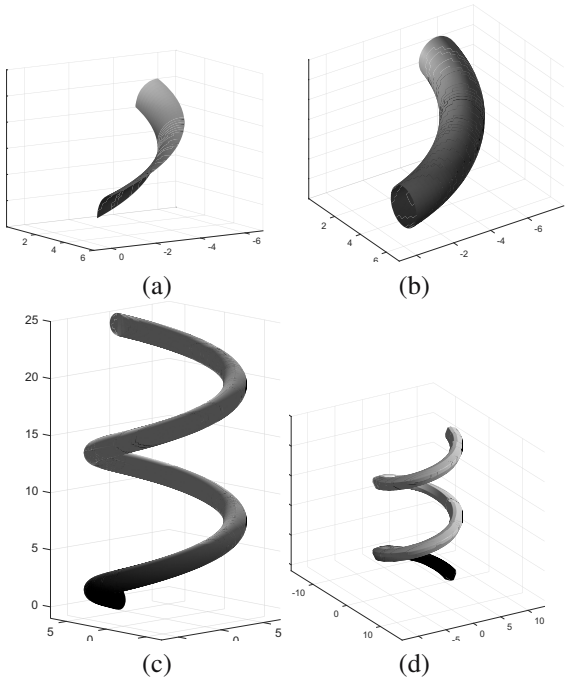

Fig. 13. Construction and deformation of the spring: the basic arc surface constructed using sixteen control points, with $\alpha = 1$ and $\beta = 1$ (a), the segment of a helical tube formed by the connection of four arc surfaces (b), a segment of a spring formed by the connection of eight helical tube segments (c), a rectangular spring, with $\alpha = 10$ (d).

matching the shape of Fig. 9(b). Adjusting the surface shape through α does not alter the control points, thus preserving continuity both within each surface patch and at the boundaries between patches.

♦

The above analysis addresses the fitting and deformation of the $\alpha\beta$-sh Bézier surface for specific surface types. Next, we present several examples to demonstrate the application of $\alpha\beta$-sh Bézier surface deformation in industrial design.

Example 10. Helical tubes are commonly used in everyday applications, particularly as springs. In mechanical equipment and the automotive industry, rectangular springs are more frequently employed. Compared to springs with circular cross-sections, rectangular springs offer greater stiffness, enhanced elasticity, and improved stability and fatigue resistance, especially under high-speed vibration.

The helical tube is created by fitting a spring using the $\alpha\beta$-sh Bézier surface, constructed by joining multiple arc segments. Figure 13(a) shows a quarter of the helical tube, and through additional segment connections, the helical tube in Fig. 13(b) is formed. By rotating this segment (Fig. 13(b), a complete spring (Fig. 13(c)) is obtained. Finally, by adjusting the parameter values, a rectangular spring, as shown in Fig. 13(d), is generated. Throughout this transformation process, the positions of the control points are preserved, ensuring that the surface maintains good continuity during deformation.

♦

Example 11. The $\alpha\beta$-sh Bézier surface, known for its excellent smoothness, can also be applied in the design of household appliances, providing both aesthetic benefits and improving the feasibility of product design. The following example of a wine glass illustrates the application of surface deformation.

When constructing the wine glass, the base, stem, and body are all formed by connecting four surfaces. The deformation process affects only the cup body. It is important to note that surface deformation is influenced by the start and end points. The control point at the rim of the cup is taken as the starting point, while the connection between the cup body and the stem serves as the endpoint, resulting in a quarter of the cup body as shown in Fig. 14(a). By increasing the control parameter, the surface is pulled toward the previous node at the endpoint in the component corresponding to β, as illustrated in Fig. 14(b).

The spatial control points of the surface shown in Fig. 14(a) are listed as follows:

$$\begin{array}{cccc}
(1,0,13) & (1,1\cdot k,13) & (1\cdot k,1,13) & (0,1,13)\\
(12,0,16) & (12,12\cdot k,16) & (12\cdot k,12,16) & (0,12,16)\\
(9,0,27) & (9,9\cdot k,27) & (9\cdot k,9,27) & (0,9,27)\\
(7,0,29) & (7,7\cdot k,29) & (7\cdot k,7,29) & (0,7,29).
\end{array}$$

♦

6. Discussion

Traditional Bézier curves and surfaces cannot represent special curves, such as circles, and any deformation of these curves or surfaces can only be achieved by changing the positions of the control points. To address these issues, this paper proposes a new basis function called the α-sh basis function, which is used in the construction of curves and surfaces. The basis functions are defined using the vector space $\{1, t, t^2, \ldots, t^{n-2}, \sinh t, \cosh t\}$, with the shape control parameter α incorporated into the functions. Curves constructed using the α-sh basis function can first be used to construct special curves, and second, curve and surface deformation can be achieved by adjusting the control points at the starting and ending positions, as well as by modifying the shape control parameter. The deformation process does not require altering the positions of the control points, making it simpler and more intuitive. Compared to previous research, the method proposed in this paper demonstrates superior performance in terms of curve and surface continuity over construction

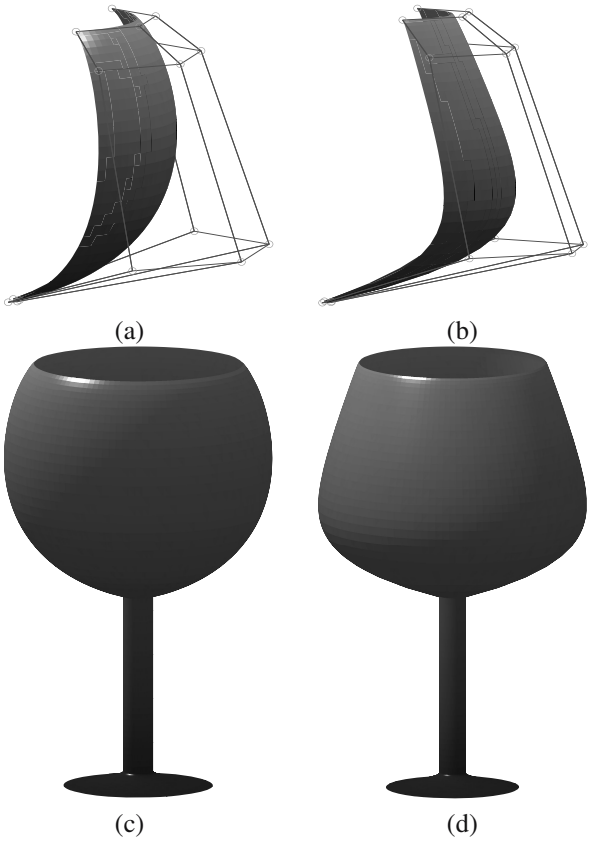

Fig. 14. Construction and deformation of wine glass: wine glass body when $\alpha = 1$, $\beta = 1$ (a), wine glass body when $\alpha = 3$, $\beta = 1$ (b), wine glass when $\alpha = 1$, $\beta = 1$ (c), wine glass when $\alpha = 3$, $\beta = 1$ (d).

methods based on trigonometric functions. When achieving higher-order continuity, the proposed method exhibits better properties and makes it easier to realize C^1 and C^2 continuity. Additionally, trigonometric functions require significantly higher computational costs when dealing with floating-point operations. Furthermore, unlike the construction methods mentioned in previous studies, the basis functions of the proposed method in this paper lack symmetry. This unique property means that the selection of the starting and ending control points also influences the deformation effect, providing more possibilities for curve and surface design. This paper also extends the application of this new construction method to both two-dimensional and three-dimensional spaces, rather than being confined to a single-dimensional space.

The use of a new basis function, compared to traditional Bézier curves and surfaces, increases the computational load, requiring more time for curve and surface construction. Additionally, during deformation, the shape control parameter must be carefully chosen. When designing curves and surfaces, special attention should be given to the distribution of control points at the starting and ending positions.

In future work, we will further investigate the deformation techniques of curves and surfaces with shape control parameters, optimize the construction method of the basis functions, and expand the ways in which parameters can control the shape.

Acknowledgment

This research was supported by the National Natural Science Foundation of China (no. 12001327).

References

Ameer, M., Abbas, M., Abdeljawad, T. and Nazir, T. (2022). A novel generalization of Bézier-like curves and surfaces with shape parameters, *Mathematics* **10**(3): 376.

Barr, A.H. (1984). Global and local deformations of solid primitives, *ACM Siggraph Computer Graphics* **18**(3): 21–30.

Bechmann, D., Bertrand, Y. and Thery, S. (1997). Continuous free form deformation, *Computer Networks and ISDN Systems* **29**(14): 1715–1725.

Farin, G., Hahmann, S., Peters, J. and Wang, W. (1987). *Geometric Modeling*, SIAM, Philadelphia.

Foley, J.D., Van Dam, A., Feiner, S.K., Hughes, J.F. and Phillips, R.L. (1994). *Introduction to Computer Graphics*, Vol. 55, Addison-Wesley, Reading.

Hsu, W.M., Hughes, J.F. and Kaufman, H. (1992). Direct manipulation of free-form deformations, *ACM Siggraph Computer Graphics* **26**(2): 177–184.

Kennard, R.W. and Stone, L.A. (1969). Computer aided design of experiments, *Technometrics* **11**(1): 137–148.

Kotan, M., Öz, C. and Kahraman, A. (2021). A linearization-based hybrid approach for 3D reconstruction of objects in a single image, *International Journal and Applied Mathematics and Computer Science* **31**(3): 501–513, DOI: 10.34768/amcs-2021-0034.

Marschner, S. and Shirley, P. (2009). *Fundamentals of Computer Graphics*, 3rd Edn, AK Peters/CRC Press, Natick.

Marschner, S. and Shirley, P. (2018). *Fundamentals of Computer Graphics*, 4th Edn, CRC Press, Boca Raton.

Maqsood, S., Abbas, M., Hu, G., Ramli, A. L.A. and Miura, K.T. (2020). A novel generalization of trigonometric bézier curve and surface with shape parameters and its applications, *Mathematical Problems in Engineering* **2020**(1): 4036434.

Mortenson, M.E. (1997). *Geometric Modeling*, John Wiley & Sons, New York.

Narayan, K.L., Rao, K.M. and Sarcar, M. (2008). *Computer Aided Design and Manufacturing*, PHI Learning Pvt, New Delhi.

Qin, X., Hu, G., Zhang, N., Shen, X. and Yang, Y. (2013). A novel extension to the polynomial basis functions describing Bézier curves and surfaces of degree n with

multiple shape parameters, *Applied Mathematics and Computation* **223**: 1–16.

Ross, D.T. and Rodriguez, J.E. (1963). Theoretical foundations for the computer-aided design system, *Proceedings of Spring Joint Computer Conference, Detroit, USA*, pp. 305–322.

Said Mad Zain, S.A.A.A., Misro, M.Y. and Miura, K.T. (2021). Generalized fractional Bézier curve with shape parameters, *Mathematics* **9**(17): 2141.

Sederberg, T.W. and Parry, S.R. (1986). Free-form deformation of solid geometric models, *Proceedings of the 13th Annual Conference on Computer Graphics and Interactive Techniques, Dallas, USA*, pp. 151–160.

Shen, W. and Wang, G. (2015). Geometric shapes of C-Bézier curves, *Computer-Aided Design* **58**: 242–247.

Wen-tao, W. and Guo-zhao, W. (2005). Bezier curves with shape parameter, *Journal of Zhejiang University—Science A: Applied Pysics & Engineering***6** (6): 497–501.

Yang, L. and Zeng, X.-M. (2009). Bezier curves and surfaces with shape parameters, *International Journal of Computer Mathematics* **86**(7): 1253–1263.

Kewei Zhang received his bachelor's degree from the School of Software Engineering, Shanxi University, Taiyuan, China, in 2019. Currently he is pursuing a master's degree at the School of Computer Science and Technology, Shandong Technology and Business University, Yantai, Shandong. His research interests include computer-aided geometric design, computation geometry and computer graphics.

Han Wang received her BS and MS degrees in applied mathematics from Inner Mongolia Minzu University, Tongliao, Inner Mongolia, China, in 2011 and 2014, respectively, and her PhD degree in computational mathematics from the Dalian University of Technology, Dalian, Liaoning, China, in 2018. She is currently a professor at the School of Computer Science and Technology, Shandong Technology and Business University. Her research interests include computer aided geometric design, computation geometry and computer graphics.

Received: 29 November 2024
Revised: 28 February 2025
Accepted: 19 March 2025